ACADEMIC PRESS

Available online at www.sciencedirect.com
SCIENCE DIRECT®

Journal of Catalysis 214 (2003) 191–199

JOURNAL OF CATALYSIS

www.elsevier.com/locate/jcat

IR study of the acidity of ITQ-2, an "all-surface" zeolitic system

B. Onida,[a,b] L. Borello,[a] B. Bonelli,[a] F. Geobaldo,[a,b] and E. Garrone [a,c,*]

[a] *Dipartimento di Scienza dei Materiali e Ingegneria Chimica, Politecnico di Torino, Corso Duca degli Abruzzi 24, I-10129 Turin, Italy*
[b] *INSTM, Unità di Ricerca Torino Politecnico, Turin, Italy*
[c] *INFM, Unità di Ricerca Torino Politecnico, Turin, Italy*

Received 18 July 2002; revised 25 October 2002; accepted 25 October 2002

Abstract

Two samples of ITQ-2 with different Al content (Si/Al = 50 and 25, respectively) and different degree of exfoliation have been characterized by IR spectroscopy and compared to MCM-22 samples with the same Al content, to assess the changes brought about by the development of a large external surface. Brønsted acidity has been measured as the propensity of OH species to either protonate ammonia or engage in H-bonds with suitable molecules (CO, N_2, *n*-heptane, olefins, aromatics). Lewis acidity has been evaluated by measuring the spectra of CO adsorbed at room temperature. Comparison with MCM-22 samples shows that no substantial loss in Brønsted acidity takes place because of exfoliation, although the bridged species Si(OH)Al exposed at the external surface do not basically survive as such and are probably converted into new AlOH acidic species. These are not directly detectable in the IR spectra; indirect evidence, however, suggests their location at the external cups of the surface. Bridged Si(OH)Al species survive instead in the 10-MR channels.

Keywords: ITQ-2; IR spectroscopy; Acidity; MCM-22

1. Introduction

Zeolite MCM-22 [1], which combines the properties and the porosity of 10-MR channels and 12-MR supercages, has opened new possibilities in catalytic processes such as alkylation of benzene to cumene [2]. A disadvantage is, however, the narrow access to the 12-MR supercages through the 10-MR openings, seriously hampering the diffusion of molecules. To avoid this limitation, a new zeolitic structure, ITQ-2, has been developed by Corma et al. [3–5], prepared by swelling and delaminating the same layered precursor, so obtaining, in principle, a house-of-cards structure of extremely thin sheets. This latter system is attracting much attention [6,7].

We have in the past studied the Brønsted and Lewis acidity of MCM-22 by following in the IR the interaction of weak Lewis bases such as CO and N_2 and unsaturated hydrocarbons [8,9]. This study is extended here to ITQ-2 and the results are contrasted with those concerning MCM-22. The purpose of the present study is twofold. On the one hand, it is of interest to gather knowledge about a very promising catalytic system. On the other hand, a wholly delaminated ITQ-2 is, in principle, an "all-surface" system: the comparison between MCM-22 and ITQ-2 may help therefore in understanding the structure of the external surface of a zeolite, a topic of substantial interest, as it has been proposed repeatedly that many catalytic reactions on zeolites occur at the outer surfaces.

Two samples of ITQ-2 have been considered, with Si/Al ratios equal to 25 and 50, to study the influence of the Al content on the properties of the solid, together with two MCM-22 samples with close Si/Al ratios, to allow comparison of the acidic properties.

2. Experimental

ITQ-2 samples have been prepared following Ref. [3], and are referred to hereafter as ITQ-2-50 (Si/Al = 50), ITQ-2-25 (Si/Al = 25), and all-silica ITQ-2 (Si/Al $\approx \infty$). XRD and BET analysis revealed that ITQ-2-25 was not completely delaminated, in agreement with the observations by Schenkel et al. [6]. MCM-22 samples, referred hereafter as MCM-22-50 (Si/Al = 50) and MCM-22-25 (Si/Al = 25), were prepared according to Refs. [10,11]. Si/Al ratios

* Corresponding author.
E-mail address: garrone@athena.polito.it (E. Garrone).

0021-9517/03/$ – see front matter
doi:10.1016/S0021-9517(02)00090-8

have been determined by elemental analysis after calcination and confirmed by energy dispersion spectroscopy (EDS) (Philips, 515 SEM equipped with EDAX 9900 EDS).

For IR measurements, self-supporting wafers were prepared and activated under dynamic vacuum (10^{-4} Torr) for 1 h at 773 K in an IR cell allowing in situ thermal treatments, gas dosage, and IR measurements both at room temperature and at a nominal temperature of 77 K, presumably in fact around 100 K. Spectra were collected on a Bruker IFS 55 Equinox instrument equipped with an MCT cryodetector working with 2 cm^{-1} resolution. During adsorption measurements, equilibration time was a few seconds with CO and N_2 and some minutes with organic compounds. When spectra of different samples are compared normalization to unit mass of the sample is used.

3. Results

3.1. OH species and interaction with ammonia

The upper part of Fig. 1 depicts the structure of MCM-22, as derived from XRD measurements [12]: both the 12-MR supercage and the 10-MR channels are clearly visible. The lower part of the figure describes the idealized structure of a sheet of ITQ-2, obtained from the structure of MCM-22 by the splitting of the supercage into two halves. This is formally accomplished by hydrolyzing each Si–O–Si linear bond with one water molecule, so that both Si atoms terminate with OH groups: no other change in geometry has been considered. The sheets are ≈2.5 nm thick and consist of a hexagonal array of 12-MR cups (arrow in the figure) that penetrate into the sheet from both sides, with an aperture of 0.7 nm. At the opposite sides of the layer they meet at the center, forming a double 6-MR window connecting the cups, bottom to bottom. The 10-MR channel system survives and runs around the cups inside the sheet [13].

Figure 2 reports the IR spectra (normalized with respect to weight) in the OH stretching region of MCM-22-25 (curve 1), ITQ-2-25 (curve 2), and ITQ-2-50 (curve 3), after outgassing at 773 K. Curve 1 shows a weak band at 3747 cm^{-1}, due to isolated SiOH species on the external surface. The tailing at lower frequencies (3730–3720 cm^{-1}) is probably due either to silanols on the internal surface or to interacting silanols, similar to those observed in silicalite [14,15]. The main peak at 3624 cm^{-1} is due to Brønsted sites Si(OH)Al; according to previous work, this band comprises both Si(OH)Al species sitting at the supercages and those located at 10-MR channels [8,9]. At both sides of the band at 3624 cm^{-1} a minor component is seen. The very weak one at 3580 cm^{-1} is due to a small fraction of Si(OH)Al species sitting at the hexagonal prisms, hardly accessible to molecules [8,9]. The weak component at 3670 cm^{-1} is the signature of Al(OH) species, the nature of which is discussed in great detail below.

On the basis of the idealized structure in Fig. 1, a substantial increase in silanol population is expected on passing from the MCM-22 sample to those delaminated, as well as a marginal change in the intensity of the Si(OH)Al species, which are in principle untouched by the delami-

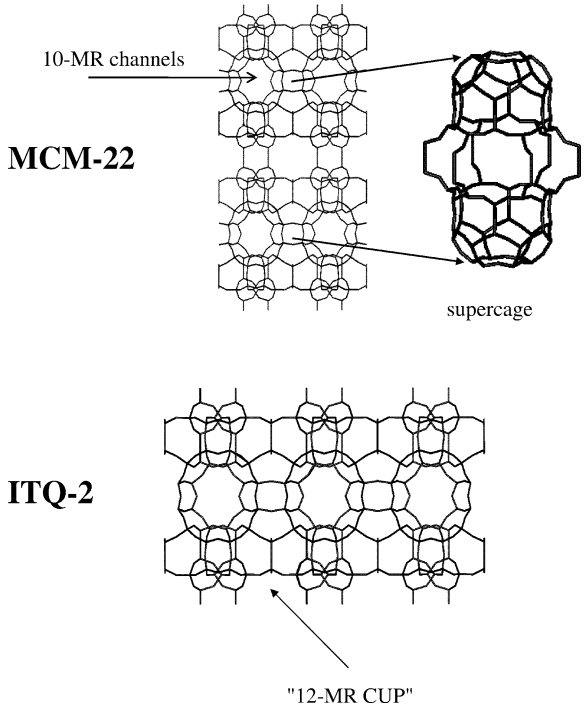

Fig. 1. Ideal structures of the zeolite MCM-22 and the layered compound ITQ-2.

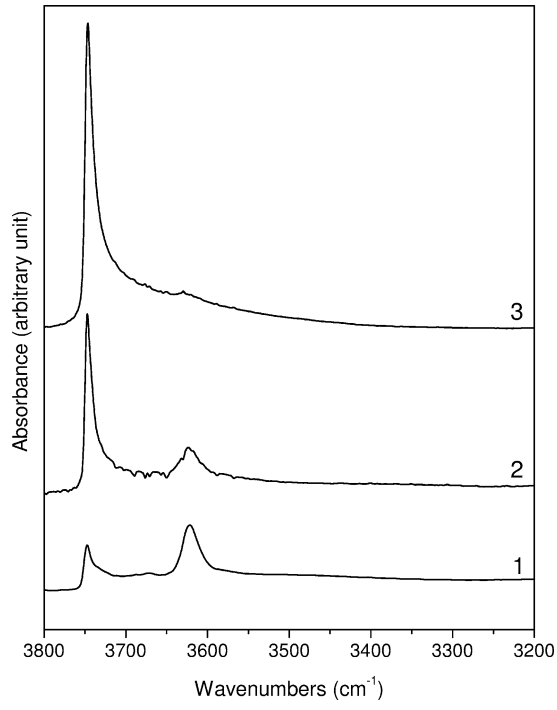

Fig. 2. IR spectra in the O–H stretching regions of MCM-22-25 (curve 1); ITQ-2-25 (curve 2); ITQ-2-50 (curve 3).

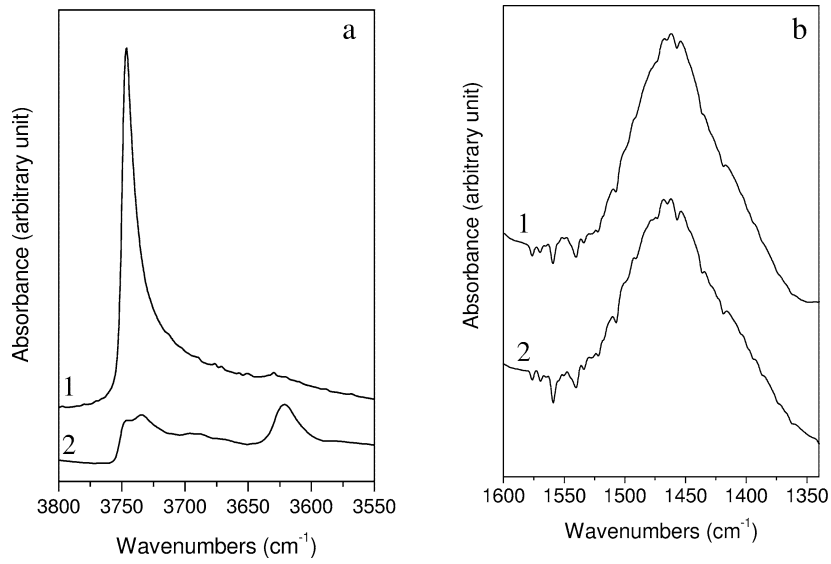

Fig. 3. Comparison of IR spectra of ITQ-2-50 (curves 1) and MCM-22-50 (curves 2). (a) The O–H stretching region of the naked samples; (b) ammonium species formation after NH_3 adsorption and evacuation at room temperature.

nation process. Curve 2 (ITQ-2-25) shows indeed a definitely more intense SiOH band. The band due to Brønsted sites is observed at the same location (3624 cm^{-1}) as with MCM-22; its intensity, though, is weaker than with MCM-22, notwithstanding the similar Al content. Curve 3 shows the same features in a yet more marked way. The SiOH absorption is very intense, the higher intensity of the SiOH peak in ITQ-2-50 with respect to ITQ-2-25 being in line with the lower degree of delamination of the latter. The band at 3624 cm^{-1} is hardly visible. Even taking into account that the Al content is about half of that of the other two samples, a definite peak is expected in the spectrum at 3624 cm^{-1}: instead, a small bump is seen, superimposed on a marked tailing of the 3747 cm^{-1} band to lower frequencies.

A direct comparison between spectra of the low Al-containing samples MCM-22-50 and ITQ-2-50, in the OH stretching region, is made in Fig. 3a. In the spectrum of MCM-22-50, peaks due to isolated silanols on the external (3747 cm^{-1}) and internal (3730 cm^{-1}) surfaces are observed. Broad absorption is visible in the range 3700–3650 cm^{-1}, due to Al(OH) species. The band at 3624 cm^{-1}, due to Si(OH)Al species, is well defined, confirming that the intensity of the same band in ITQ-2-50 is much lower than expected on the basis of the aluminum content.

A possible reason for the decrease of the 3624 cm^{-1} band is dealumination, i.e., the loss of framework Al because of thermal treatments. Figure 3b shows that this is presumably not so by comparing the spectra of MCM-22-50 and ITQ-2-50 after adsorption of ammonia and successive evacuation at room temperature for 2 h. The intensity of the band at 1465 cm^{-1} due to ammonium species is nearly the same in the two spectra; as the related extinction coefficient may be reasonably assumed to be fairly constant for similar solids and adsorption centers, it results that, although not readily visible in the spectrum of ITQ-2-50, acidic OH species are present, able to transfer their protons to ammonia, and the number of Brønsted sites is basically unchanged. The experiment in Fig. 3b also suggests, within the limits of validity of the assumption of a constant extinction coefficient for the ammonium species, that the loss of acidic Brønsted sites due to dealumination is limited; further support for this is provided below.

Acidity of Brønsted sites for all samples has been measured by the extent of the shift imparted by several molecules to the OH-stretching mode. CO and N_2 adsorption has been carried out at a nominal temperature of 77 K. Ethylene and propene adsorption has been carried out both at room temperature and at a temperature in the range 100–150 K. In the case of ITQ-2-50, this latter experiment gives rise to better-defined bands and for this reason corresponding data will be considered. Benzene, toluene, and 1,3,5-trimethylbenzene have been studied at ambient temperature.

3.2. Interaction with CO and N_2

Figure 4 reports as difference spectra the changes in the OH stretching region brought about by the adsorption of CO and N_2 on ITQ-2-50 (solid curves). The broken curve refers to the all-silica ITQ-2, used as a reference. The body of the figure refers to CO adsorption and the inset to N_2 adsorption. Arrows indicate changes in the spectrum with increasing pressure; negative bands indicate species decreasing in intensity along the experiment.

In all spectra a sharp positive peak occurs at 3751 cm^{-1} (accompanied by a negative signal at 3747 cm^{-1}) which increases with pressure; this is a merely physical effect, in

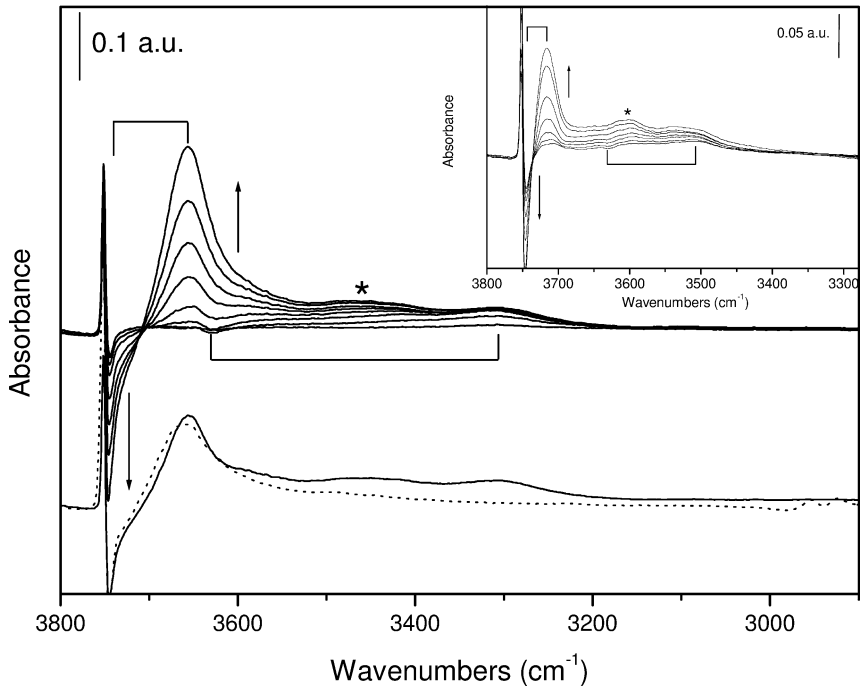

Fig. 4. Difference IR spectra concerning the adsorption of CO on ITQ-2-50 at nominal 77 K ($10^{-2} < p < 13$ mbar). The O–H stretching region is shown (the broken curve refers to the all-silica ITQ-2 reported for comparison). Inset: the same experiment run with N_2 ($10^{-2} < p < 40$ mbar). Arrows indicate increasing pressure. Forks connect corresponding negative and positive peaks; the asterisk labels the band due to X–OH species (see text).

that the SiOH mode shifts to higher frequency because of the decrease in the sample temperature [16], due to the thermal conduction of CO and N_2, which is higher the larger the pressure.

Let as consider first the central part of the figure: at low CO coverages, an absorption appears at about 3300 cm^{-1} accompanied by a weak negative peak at 3628 cm^{-1}, related to the interaction of Si(OH)Al species with CO. The observed shift (328 cm^{-1}) is the same measured for the same species in MCM-22 [8]. At higher CO coverages, new absorptions appear at about 3460 and 3660 cm^{-1}, and a negative peak increases at 3749 cm^{-1}, with a tailing at lower frequencies.

The broad band at about 3660 cm^{-1} is due to SiOH species H-bonded to CO, the stretching mode of which is shifted from 3749 by about 90 cm^{-1}, as observed with Aerosil [17]. The broken curve in the lower part of the figure concerns the all-silica ITQ-2 outgassed in similar circumstances and contacted with CO at low temperature. For comparison, this broken curve is superimposed on the appropriate curve of the central portion. The two curves coincide as far as the interaction of CO with SiOH species is concerned (positive band at 3660 cm^{-1}, negative peak at 3749 cm^{-1}), whereas the two bands at 3460 and 3300 cm^{-1} only feature in the spectrum of the Al-containing ITQ-2 sample, thus proving to be related to Al species.

The band growing at 3460 cm^{-1} (asterisk) is not paired to any negative peak. On the basis of its frequency and its appearance at higher pressures with respect to the 3300 cm^{-1} band, it is ascribable to a species less acidic than Si(OH)Al but nonetheless definitely more acidic than SiOH; these species are indicated hereafter as X–OH.

Similar results are obtained with N_2 (inset): the peaks due to Si(OH)Al and silanol species are shifted, as expected, by about 120 cm^{-1} (positive band at about 3510 cm^{-1}) and 40 cm^{-1} (positive band at about 3710 cm^{-1}), respectively [18,19]. A band appears at about 3600 cm^{-1} (asterisk), again not paired to any negative peak and ascribed to the same X–OH species.

Figure 5 reports the same spectra as in Fig. 4 in the CO stretching region. At low coverage three peaks are seen at 2243, 2230, and 2176 cm^{-1}. The two peaks above 2200 cm^{-1} are due to two types of exposed Lewis acidic centers involving Al^{3+} cations: the band at 2230 cm^{-1} is often observed in calcined zeolites [16,18]. The peak at 2176 cm^{-1} is due to CO molecules interacting with Si(OH)Al species, its frequency being the same as that observed for the Si(OH)Al species in MCM-22 [8].

With the increase of CO pressure, the band due to CO interacting with Si(OH)Al species increases: new bands appear at 2156 and 2138 cm^{-1}, due to CO interacting with silanols and in a liquid-like phase, respectively. A new shoulder also appears at 2165 cm^{-1} (asterisk), due to CO molecules interacting with species with acidity intermediate between silanols and Si(OH)Al species, i.e., the X–OH species.

As to CO species bonded to Lewis sites, the intensity of the peaks at 2243 and 2230 cm^{-1} increases only slightly

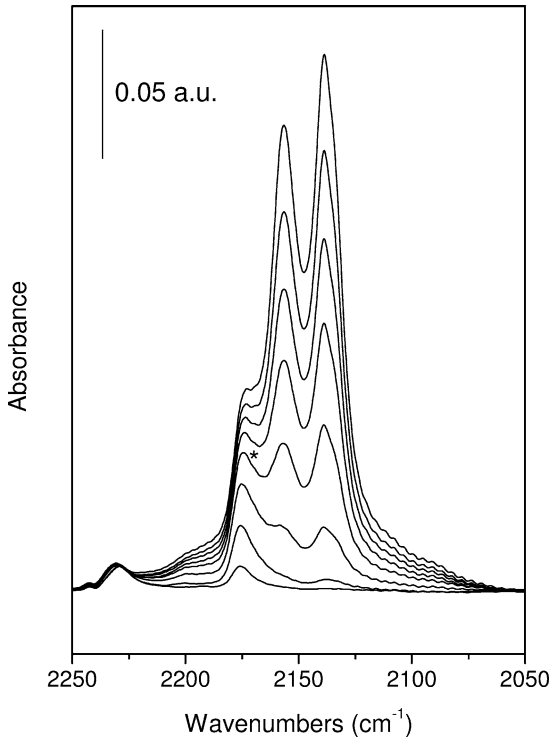

Fig. 5. Difference IR spectra concerning the adsorption of CO on ITQ-2-50 at nominal 77 K ($10^{-2} < p < 13$ mbar) in the CO stretching region. The asterisk labels the band due to X–OH species (see text).

with increasing CO pressure: a small shift to higher frequencies is observed for the latter peak, not discussed here. Taking into account that, in the absence of back donation, as in this case, the extinction coefficient of the CO stretching mode does not vary much with frequency [20], the low intensity of both peaks at 2243 and 2230 cm^{-1} with respect to the intensity of the bands at 2176 and 2165 cm^{-1}, due to Si(OH)Al and X–OH species, suggests that the population of Lewis sites is small with respect to that of Brønsted sites. This supports the idea that dealumination is not the main reason for disappearance of the 3624 cm^{-1} band in the spectrum of ITQ-2-50, in agreement with NMR data reported by Schenkel et al. [6], which show a small increase of the signal due to octahedral aluminum when passing from MCM-22 to ITQ-2.

3.3. Other bases (olefins and aromatics)

For brevity, data are not reported as figures, and results are gathered in Table 1. Findings similar to those just described are obtained, in that three types of bands are observed in the interactions: (i) bands due to Si(OH)Al species; (ii) bands due to interacting silanols; (iii) bands at frequencies between those of silanols and those of Si(OH)Al species, assigned to H-bonded X–OH species.

In particular, adsorption of 1,3,5-trimethylbenzene (TMB) has been carried out to gain information about the location of X–OH species, because this molecule cannot diffuse inside the 10-MR channels, and is therefore probably adsorbed exclusively on the external surface. Figure 6 reports the results of the experiment as difference spectra. Besides the CH stretching modes in the range 3100–2800 cm^{-1}, two absorptions are observed: an intense band at 3570 cm^{-1} and a broad absorption centered at 3370 cm^{-1}. The former is due to silanols interacting with the aromatic ring. The shift (167 cm^{-1}) is larger than that observed with benzene (120 cm^{-1}), because of the higher basicity of the aromatic ring of TMB, due to the + I inductive effect of the methyl substituents.

Table 1
Shifts $\Delta\nu_{OH}$ of the OH stretching mode of SiOH, X–OH, and Si(OH)Al species in ITQ-2: for X–OH species frequencies observed for the H-bonded adduct are reported and related shifts are calculated assuming 3760 cm^{-1} as the frequency of the free hydroxyl

	$\Delta\nu$ [SiOH]	ν [XOH]	$\Delta\nu$ $[XOH]_{3670}$	$\Delta\nu$ [Si(OH)Al]
N_2	40[a]	3600[a]	70[a]	120[a]
n-Heptane	48	3570	100	145
CO	90[a]	3460[a]	210[a]	330[a]
C_2H_4	104; 140[b]	3360[b]	310[b]	390; 426[b]
C_3H_6	153; 190[b]	3260[b]	410[b]	480; 526[b]
C_6H_6	120	3420	250	310
C_7H_8	147	–	–	360
1,3,5 TMB	167	3370	300	–

[a] 100 K.
[b] 100 K < T < 150 K.

The frequency of the latter band (3370 cm^{-1}) is 50 cm^{-1} lower than that of the band observed for the X–OH species in the interaction with benzene (Table 1), and is accordingly assigned to X–OH species interacting with TMB.

As it concerns Si(OH)Al species, on the basis of their behavior with the other probes, the absorption due to these species when interacting with TMB is expected below 3250 cm^{-1}. A weak component is indeed visible in this region, weaker than that related to X–OH species. This could be evidence for the survival of some Si(OH)Al species at the outer surfaces. It has, however, to be noted that the presence of the component at 3250 cm^{-1} resides on a small negative bump at 3210 cm^{-1} (asterisk), which, instead of being the valley between two peaks, could be an artefact due to an "Evans window" [21], arising from the Fermi resonance between the overtone of the intense TMB ring vibration at 1606 cm^{-1} and the tailing of the broad band at 3570 cm^{-1}. In this latter hypothesis, little or no interaction would occur between TMB and Si(OH)Al species at the external surfaces. On the other hand, spectra related to ITQ-2-25 (inset in Fig. 6) clearly show that the adsorption of TMB does not perturb the band at 3624 cm^{-1}, suggesting that visible Si(OH)Al species are located mainly on the internal surface (10-MR channels and perhaps residual 12-MR supercages). In conclusion, the population of Si(OH)Al species at the outer surfaces of ITQ-2, if any, is limited, and accordingly, only a very weak negative signal can be observed at 3624 cm^{-1} in the first spectrum in Fig. 6 (arrow).

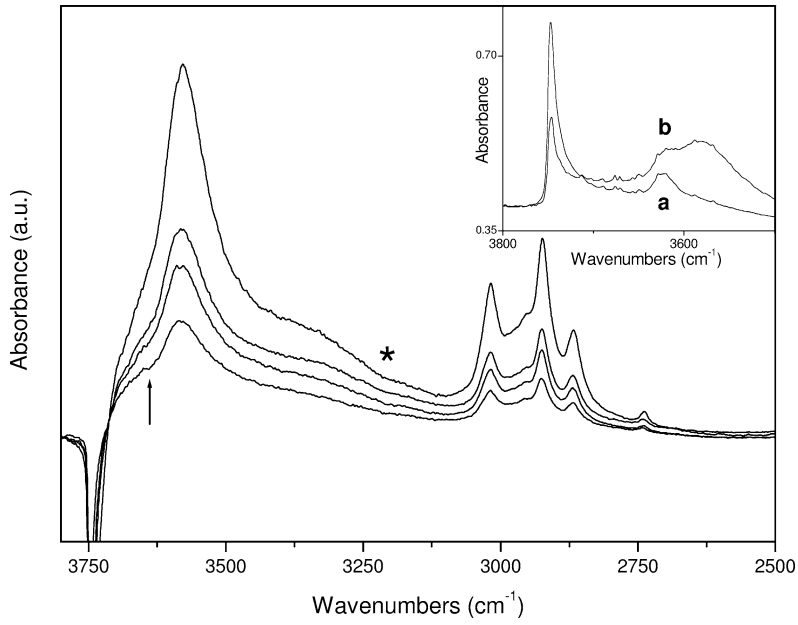

Fig. 6. IR spectra concerning the adsorption of TMB on ITQ-2-50 (body of the figure) and ITQ-2-25 (inset). Body: difference spectra at increasing amounts of TMB. Arrow: possible occurrence of Si(OH)Al species as a negative band. Asterisk: possible Evans window (see text). Inset: curve a, naked sample; curve b, adsorption of TMB.

4. Discussion

4.1. Brønsted sites

Delamination of MCM-22 causes an increase of the silanol population, as expected, and a decrease of the Si(OH)Al species responsible of the band at 3624 cm^{-1}. The interaction with basic probes shows that in ITQ-2 these species are the same as those observed in MCM-22, in terms of both acidity and accessibility. Their acidity is strong and similar to that observed with most low-aluminum zeolites (ZSM-5, beta, mordenite) and they are most probably located in the internal surface, i.e., in 10-MR channels.

The overall Brønsted acidity as measured by the ability to protonate ammonia does not decrease upon delamination. This is in agreement with data reported by Schenkel et al. concerning pyridine adsorption [6]. The reason is probably the formation of new OH species, designated so far as X–OH (which compensates for the loss of Si(OH)Al species), the acidity of which is strong enough to protonate ammonia, but is lower than that of Si(OH)Al species, as H-bonded X–OH species are formed systematically at higher pressure of any basic probe with respect to Si(OH)Al species. Support to this comes from the stretching frequency of CO interacting with X–OH species, 2165 cm^{-1}, as opposed to 2176 cm^{-1}.

In order to measure precisely the acidity of X–OH species, the set of shifts $\Delta\nu_{OH}$ with the different probes have to be defined, which implies assuming a value for the frequency of free hydroxyls. No definite signal ascribed to unperturbed X–OH is visible in the spectrum of ITQ-2: only a broad tail in the range 3700–3400 cm^{-1} is observed in the spectrum of the bare sample, and even difference spectra related to adsorption of probes do not show any definite component. Lavalley and co-workers reported a similar result, concerning adsorption of CO on steamed and leached Y faujasites [16], where a band was observed at 3465 cm^{-1} in the presence of adsorbed CO, not associated with any evident peak in the spectrum of the naked sample.

To investigate the nature of the X–OH species, and to assess the frequency of the related O–H stretch in the free species, we have compared the CO spectra of ITQ-2-50 and those concerning a steamed MCM-22 sample with $Si/Al = 14$ (Fig. 7) [8]. This latter has two acidic species, i.e., the Si(OH)Al species which survived steaming, and a species AlOH responsible for a band at 3670 cm^{-1}, directly observable in the inset and as a negative band in the figure (arrows). In the CO adsorption experiment, two positive bands are accordingly seen, one at 3310 cm^{-1}, due to Si(OH)Al species, and a band at 3465 cm^{-1}, corresponding to the AlOH species at 3670 cm^{-1}. The spectrum of ITQ-2-50 (broken curve) also shows these two bands due to H-bonded hydroxyls. Moreover, the stretching frequency of CO molecules interacting with species responsible for the 3670 cm^{-1} band is at 2165 cm^{-1} [8], the same frequency observed for CO interacting with X–OH species in ITQ-2. In conclusion, a value of 3670 cm^{-1} appears to be a reasonable candidate for the frequency of free X–OH, though not directly observed, and we assume that the X–OH species may coincide with the AlOH species responsible for that band.

Absorption at 3670 cm^{-1} is often observed in zeolite spectra and generally assigned to hydroxyls linked to extraframework Al species. Most authors consider such species

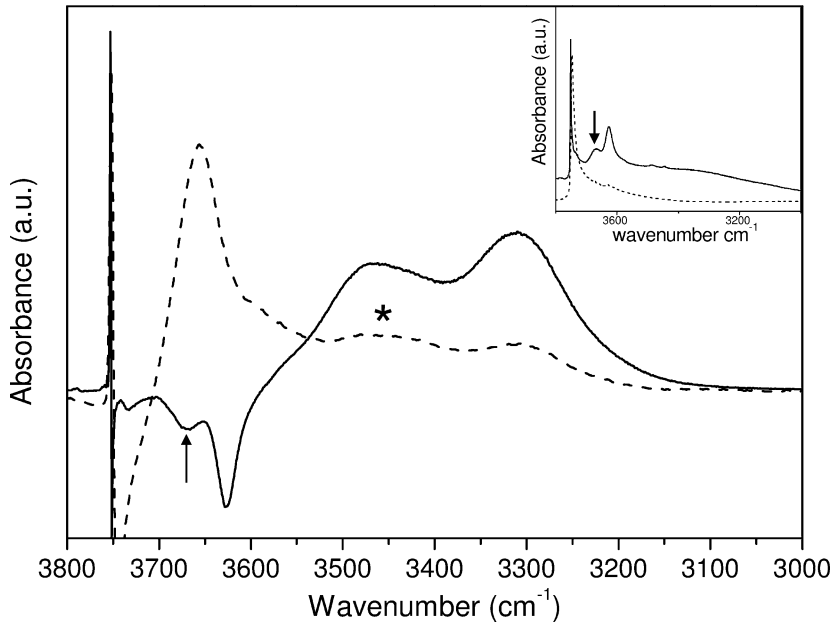

Fig. 7. IR spectra concerning the comparison of ITQ-2-50 (broken curves) and a steamed MCM-22 sample (solid curves). Body: adsorption of CO at nominal 77 K. Inset: comparison of the OH stretching regions of the naked samples. Arrows: location of the AlOH band at 3670 cm^{-1}.

as an AlOH group sitting on aluminum oxide clusters formed by dealumination during calcinations or steaming [22,23]. The acidity observed for this species, however, as measured by $\Delta\nu_{OH}$ values, is by far larger than that of any OH species on alumina [24]. This consideration has led to an alternative interpretation, according to which AlOH species are structural defects arising from dealumination, but still anchored to the zeolitic framework [25–27]. Additional evidence supporting this interpretation comes from the study of SAPO-5 zeotype (a system not subjected to dealumination), which also exhibits a similar band, suffering the same shift with CO [28]: similar AlOH species might form readily on the surface and/or in correspondence to defects of SAPO crystals.

It cannot be ruled out, however, that bands occasionally observed in the same region are actually due to OH on aluminum oxides. In this case, they should exhibit very low acidity.

The formation upon exfoliation of AlOH species similar to those formed in zeolites by incipient dealumination is not surprising, because both the treatment in HCl solutions during the exfoliation of the layered precursor and the following calcinations [3] are likely to bring about hydrolysis of Si–O–Al bonds. As shown by TMB adsorption, Al–OH species are located on the surface of layers, i.e., on the "new" external surface produced by exfoliation. Thus, it can be proposed that Si(OH)Al species located in 12-MR supercages of original MCM-22 are precursors of the new Al–OH species in the exfoliated material.

The question to be addressed is why the AlOH species in ITQ-2 are not visible in the IR as such, but only through the interactions with basic probes as H-bonded species. Indeed, a broad tail between 3700 and 3600 cm^{-1} is observed in the OH spectrum of naked fully delaminated ITQ-2-50 (Fig. 2), which could indicate that the O–H vibration of AlOH is smeared out, not yielding a definite band. The reason for this spreading might be some structural heterogeneity, due to the fact that these species are not proper framework hydroxyls, but rather defects. Moreover, some AlOH species might be in interaction with neighbor species, such as SiOH (as described in Scheme 1), thus inducing further heterogeneity. It may be assumed that when interaction with a basic probe occurs, AlOH species, transformed into AlO–H···B complexes, are affected by the above factors to a lesser extent, so that heterogeneity is reduced in H-bonded species and a definite absorption is visible. Moreover, the extinction coefficient of H-bonded hydroxyls is always higher than that of free hydroxyls.

Scheme 1 proposes a mechanism for the formation of AlOH species from the bridged Si(OH)Al species (species *a*), which is an extension of that proposed by Zecchina and Otero Areán for the formation of the Lewis site in zeolites [18]: it consists in a water-mediated rearrangement (through elimination and readsorption of water) of the surroundings of the Al atom, yielding first the Lewis site species *b*, then Brønsted species. Two possible mechanisms of water readsorption on the Lewis site may be envisaged. In the former (right hand side reaction), a water molecule is chemisorbed in a dissociative way, yielding one SiOH and one AlOH species (species *c*). This latter, resulting from the cleavage of one Al–O bond, should have Al in trigonal coordination. This type of coordination is not common for Al: moreover, such hypothetical trigonal Al species should exhibit, besides Brønsted acidity of the terminal proton, Lewis acidity, e.g., toward CO. Data discussed below suggest that this is not so. We assume therefore that addi-

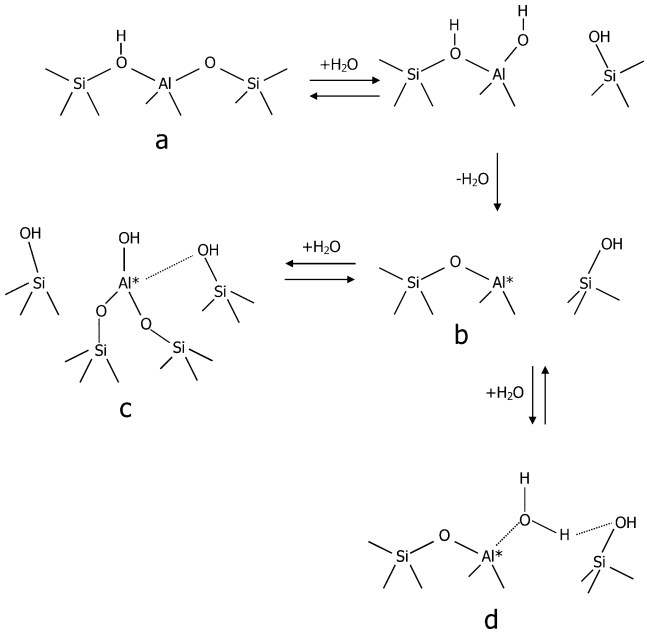

Scheme 1.

tional interactions between the Al^{3+} center and neighbor silanols (evidenced by the broken line in Scheme 1) may shield the site, preventing the Lewis acid–base adduct with CO from being formed.

Alternatively (downward reaction, yielding species *d*), a water molecule is adsorbed onto the Lewis site in a nondissociative way, giving rise to acidic Al–OH species, similar to those invoked to explain the acidity of clays.

On the basis of the present data, it is not possible to propose a definite choice between the two alternatives.

4.2. Lewis sites

Two sites have been observed by CO adsorption, with bands at 2230 and 2243 cm^{-1}. The former species is likely to coincide with species *b* in Scheme 1, as interconversion between the CO species at 2230 cm^{-1} and the OH band at 3670 cm^{-1} has been observed. Indeed, with MCM-22 steaming gives rise to the 3670 cm^{-1} band at the expense of the CO band at 2230 cm^{-1}. With ITQ-2-25 outgassed for a short time, a band at about 3670 cm^{-1} has been occasionally observed (spectra not reported), without adsorption of CO revealing any peak at 2230 cm^{-1}: prolonged outgassing (removal of chemisorbed water?) led to disappearance of the 3670 cm^{-1} band in the spectrum of the naked sample and the appearance of the 2230 cm^{-1} bond upon adsorption of CO.

This strongly suggests that the band at 2230 cm^{-1} observed with CO is due to Lewis sites, which can be converted, in the presence of water, into Brønsted sites with stretching frequency around 3670 cm^{-1}.

The CO peak at 2243 cm^{-1} is indicative of very strong Lewis sites, being as high in frequency as the strongest sites observed on alumina, implying the most coordinatively unsaturated Al^{3+} cations [22]. On this basis it is assigned to Al^{3+} ions in small aluminum oxide clusters formed by complete dealumination [23].

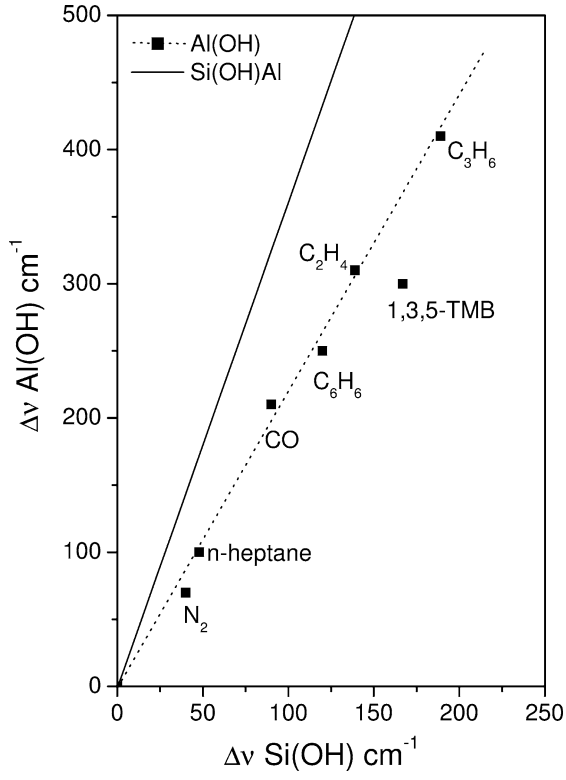

Fig. 8. BHW plot for the AlOH species in ITQ-2-50 as compared with the isolated silanol in Aerosil. Solid line: reference MCM-22 system.

4.3. Acidity of AlOH species

Comparison of the acidity of different species by spectroscopic means is usually carried out in solution or in the gas phase through the Bellamy–Hallam–Williams plot. The shifts undergone by two different hydroxyls with the same set of base molecules are plotted one against the other: a straight line passing through the origin is obtained, the slope of which is a measure of the relative acidity. Figure 8 reports such a BHW plot for the AlOH species (broken line) by assuming as independent variables the shifts observed for the isolated silanol species. The full line represents schematically the data for the Si(OH)Al species of MCM-22 [9], and it is reported for comparison. The marked difference in slope evidences the lesser acidity of the AlOH species with respect to Si(OH)Al groups. The former, though, can give a proton transfer to ammonia. Together with the residual Si(OH)Al species, they are likely to be responsible for the catalytic properties of ITQ-2. This has been interpreted as a balanced combination of acid strength higher than that of Al/MCM-41 and silica–aluminas and accessibility of acidic sites easier than for microporous zeolites [7,29].

In Fig. 8, the point related to TMB does not lie on the straight line, in that the corresponding shift is smaller than expected. Similar behavior has been observed for

the same molecule in SAPO-40 and for other relatively bulky molecules in different zeolites (ZSM-5, MCM-22, THETA-1), and it has been ascribed to the fact that such molecules do not display optimal H-bonding with the acidic species, because of secondary interactions with the zeolitic walls around the site [30]. This indicates that AlOH species are located inside zeolitic-like cavities and not on flat amorphous surfaces like that of Aerosil, in full agreement with the existence of 12-MR cups on the external surface of ITQ-2 [13].

5. Conclusions

Exfoliation is not complete with the ITQ-2-25 sample, whereas it is probably so with the sample more dilute in Al. Accordingly, a significant number of bridged Brønsted species survive in ITQ-2-25 with unaltered features. Instead, on much delaminated samples, probably exhibiting mostly outer surfaces, Si(OH)Al species are severely reduced in number. Brønsted acidity survives, because at the outer surfaces Si(OH)Al species are transformed into AlOH species, still anchored to the zeolitic framework and considerably acidic, thus able to protonate ammonia, but suffering smaller shifts in the OH stretching mode by the interaction with a probe. A mechanism similar to that proposed for incipient dealumination in zeolites may account for the formation of these new AlOH species, which are not visible directly in the IR spectra, but only in the interactions with probe molecules. The experiment with TMB seems to confirm their location at the external 12-MR cups. Together with residual Si(OH)Al species, located mainly in 10-MR channels, they may be responsible for the catalytic efficiency of ITQ-2.

Acknowledgments

We thank Dr. Flaviano Testa for sample preparation and ASI (Agenzia Spaziale Italiana) for financial support (ZEUS project).

References

[1] M. Leonowicz, J.A. Lawton, S.L. Lawton, M.K. Rubin, Science A 264 (1994) 1910.
[2] G. Sastre, C.R.A. Catlow, A. Corma, J. Phys. Chem. B 103 (1999) 5187.
[3] A. Corma, V. Fornés, S.B. Pergher, T.L.M. Maesen, Nature 393 (1998) 356.
[4] A. Corma, V. Fornés, J. Martínez-Triguero, S.B. Pergher, J. Catal. 186 (1999) 57.
[5] A. Corma, U. Diaz, V. Fornes, J.M. Guil, J. Catal. 191 (2000) 218.
[6] R. Schenkel, J.-O. Barth, J. Kornatowski, J.A. Lercher, Stud. Surf. Sci. Catal. 142 (2002) 69.
[7] A. Corma, V. Fornés, Stud. Surf. Sci. Catal. 135 (2001) 73.
[8] B. Onida, F. Geobaldo, F. Testa, F. Crea, E. Garrone, Microporous Mesoporous Mater. 30 (1999) 119.
[9] B. Onida, F. Geobaldo, F. Testa, R. Aiello, E. Garrone, J. Phys. Chem. 130 (2000) 2951.
[10] A. Corma, C. Corell, P. Pérez-Pariente, Zeolites 15 (1995) 2.
[11] Y.J. He, G.S. Nivarthy, F. Eder, K. Seshan, J.A. Lercher, Micropor. Mesopor. Mater. 25 (1998) 207.
[12] M.E. Leonowitz, J.A. Lawton, S.L. Lawton, M.K. Rubin, Science 264 (1994) 1910.
[13] A. Corma, V. Fornés, M.S. Galletero, H. García, J. Gómez-García, Phys. Chem. Chem. Phys. 3 (2001) 1218.
[14] A. Zecchina, S. Bordiga, G. Spoto, L. Marchese, G. Petrini, G. Leofanti, M. Padovan, J. Phys. Chem. 96 (1992) 4985.
[15] M. Trombetta, G. Busca, S.A. Rossigni, V. Piccoli, U. Corsaro, J. Catal. 168 (1997) 349.
[16] O. Cairon, T. Chevreau, J.C. Lavalley, J. Chem. Soc. Faraday Trans. 94 (1996) 3039, and references therein.
[17] G. Ghiotti, E. Garrone, C. Morterra, F. Boccuzzi, J. Phys. Chem. 83 (1979) 2863;
T.P. Beebe, P. Gelin, J.T. Yates, Surf. Sci. 148 (1984) 526.
[18] A. Zecchina, C. Otero Areán, Chem. Soc. Rev. (1996) 187, and references therein.
[19] F. Wakabayashi, J. Kondo, A. Wada, K. Domen, C. Hirose, J. Phys. Chem. 97 (1993) 10761.
[20] V. Bolis, B. Fubini, E. Garrone, C. Morterra, P. Ugliengo, J. Chem. Soc. Faraday Trans. 88 (1992) 391.
[21] G.C. Pimentel, A.L. McClellan, The Hydrogen Bond, Freeman, San Francisco, 1960.
[22] M. Trombetta, T. Armaroli, A.G. Alejandre, J.R. Solis, G. Busca, Appl. Catal. A Gen. 192 (2000) 125, and references therein.
[23] G. Catana, D. Baetens, T. Mommaerts, R.A. Schoonheydt, B.M. Weckhuyesen, J. Phys. Chem. 105 (2001) 4904, and references therein.
[24] C. Morterra, G. Magnacca, Catal. Today 27 (1996) 497.
[25] L.M. Kustov, V.B. Kasansky, S. Beran, L. Kubelková, P. Jiru, J. Phys. Chem. 91 (20) (1987) 5247.
[26] E. Garrone, R. Chiappetta, G. Spoto, P. Ugliengo, A. Zecchina, F. Fajula, in: R. von Ballmoos, et al. (Eds.), Proc. of the 9th International Zeolite Conference, Montreal, 1993, p. 267;
A. Zecchina, S. Bordiga, G. Spoto, D. Scarano, G. Petrini, G. Leofanti, M. Padovan, C. Otero Areán, J. Chem. Soc. Faraday Trans. 88 (1992) 2959.
[27] S. Kotrel, J.H. Lunsford, H. Knözinger, J. Phys. Chem. 105 (2001) 3917.
[28] B. Onida, PhD thesis, Politecnico di Torino, 1998.
[29] A. Corma, H. García, J. Miralles, Micropor. Mesopor. Mater. 43 (2001) 161.
[30] B. Onida, B. Bonelli, L. Borello, S. Fiorilli, F. Geobaldo, E. Garrone, J. Phys. Chem. B 106 (2002) 10518.